Electron spin resonance shifts in $S = 1$ antiferromagnetic chains

Shunsuke C. Furuya,[1] Yoshitaka Maeda,[2] and Masaki Oshikawa[3]
[1]*DPMC-MaNEP, University of Geneva, 24 Quai Ernest-Ansermet CH-1211 Geneva, Switzerland*
[2]*Analysis Technology Center, Fujifilm Corporation, Kanagawa 250-0193, Japan*
[3]*Institute for Solid State Physics, University of Tokyo, Kashiwa 277-8581, Japan*
(Received 29 August 2012; published 15 March 2013)

We discuss electron spin resonance (ESR) shifts in spin-1 Heisenberg antiferromagnetic chains with a weak single-ion anisotropy, based on several effective field theories: the O(3) nonlinear sigma model (NLSM) in the Haldane phase, free-fermion theories around the lower and the upper critical fields. In the O(3) NLSM, the single-ion anisotropy corresponds to a composite operator which creates two magnons at the same time and position. Therefore, even inside a parameter range where free magnon approximation is valid for thermodynamics, we have to take interactions among magnons into account in order to include the single-ion anisotropy as a perturbation. Although the O(3) NLSM is only valid in the Haldane phase, an appropriate translation of Faddeev-Zamolodchikov operators of the O(3) NLSM to fermion operators enables one to treat ESR shifts near the lower critical field in a similar manner to discussions in the Haldane phase. Our theory gives quantitative agreements with a numerical evaluation using quantum Monte Carlo simulation, and also with recent ESR experimental results on a spin-1 chain compound $Ni(C_5H_{14}N_2)_2N_3(PF_6)$.

DOI: 10.1103/PhysRevB.87.125122 PACS number(s): 76.20.+q, 75.10.Jm, 75.30.Gw

I. INTRODUCTION

Quantum phase transition has been studied for a long time. In quantum magnetism, the magnetic field is the most familiar parameter to cause quantum phase transitions. An $S = 1$ Heisenberg antiferromagnetic (HAF) chain and an $S = \frac{1}{2}$ two-leg HAF ladder are typical examples of one-dimensional quantum spin systems which show quantum phase transitions induced by the magnetic field. These systems have the unique ground state separated from excited states by a finite excitation gap, at zero field. As the magnetic field is gradually applied, the excitation gap is going to vanish.[1,2] After the collapse of the excitation gap, the system enters into a field-induced critical phase. The field-induced critical phase lies in a range $H_{c1} < H < H_{c2}$. Here, H_{c1} and H_{c2} are called as a lower and an upper critical field. For $H < H_{c1}$, the system is in the gapped phase. And for $H_{c2} < H$, the system is in another gapped phase where the spins are fully polarized. H_{c2} is also called as a saturation field.

The quantum phase transitions at $H = H_{c1}$ and H_{c2} bring about reconstructions of the excitation spectrum. Especially, dynamical properties of low-energy excitations are dramatically changed. Recently, dynamics of electron spins in the field-induced critical phases are actively investigated by various experimental techniques.[3–5] Among these experimental techniques, electron spin resonance (ESR) occupies a unique position in its sensitivity to interactions between electron spins. In fact, thanks to this advantage of ESR, many interesting ESR experiments have been performed in one-dimensional quantum spin systems under high magnetic field.[4–6] These recent precise ESR experiments highlight the necessity of reliable quantitative theory of ESR in the field-induced critical phase.

Despite the theoretical and experimental importance of the field-induced critical phase, ESR in the field-induced critical phase is less studied by theorists. This situation is in contrast to the fact that $S = \frac{1}{2}$ HAF critical chain whose low-temperature ESR is well understood.[7–10] Although ESR of the $S = 1$ HAF chain has been studied in several works, they were mostly concerned with ESR in gapped phases.[11,12] It is the objective of this paper to fill this gap by developing a theory of ESR in the field-induced critical phase, especially around quantum critical points, of one-dimensional quantum spin systems in an organized manner.

In this paper, we consider an $S = 1$ HAF chain with a general form of a single-ion anisotropy

$$\mathcal{H} = J\sum_j \boldsymbol{S}_j \cdot \boldsymbol{S}_{j+1} - g_e\mu_B H \sum_j S_j^z + D\sum_j \left(S_j^p\right)^2 + E\sum_j \left[\left(S_j^q\right)^2 - \left(S_j^r\right)^2\right] \quad (1)$$

in the whole range of the magnetic field, from zero field $H = 0$ to the saturation field $H = H_{c2}$. p, q, and r refer to the principal axes of the single-ion anisotropy. g_e and μ_B are Landé g factor of electron spin and μ_B is the Bohr magneton. We put $\hbar = k_B = g_e\mu_B = 1$ unless otherwise stated. In particular, we focus on a shift of the resonance frequency (ESR shift) caused by weakly anisotropic spin-spin interactions.

We reported, in our preceding Rapid Communication,[13] that the ESR shift in the range $H \lesssim H_{c1}$ is well explained by the so-called form factor perturbation theory[14] (FFPT) around an integrable field theory. In the case of $S = 1$ HAF chain, the O(3) nonlinear sigma model (NLSM) plays the role of the unperturbed integrable field theory in FFPT. In the Rapid Communication,[13] we applied the FFPT to the analysis of the ESR shift in $H \approx 0$ and H_{c1}, where we utilized a close relation of effective field theories in two different regions $H \approx 0$ and H_{c1}. This paper is also intended to take a closer look at this remarkable feature.

In the next section, we will briefly review a general framework of perturbative treatments for the ESR shift. We consider ESR shifts in three regions: the low-field gapped region (Sec. IV); the region near the lower critical field (Sec. V); and the region near the upper critical field (Sec. VI). In each region, we introduce an effective field theory and

apply it to the analysis of the ESR shift at low temperature. Section VII is devoted to a comparison of our theory with recent ESR experiments[5] of the $S = 1$ HAF compound NDMAP. In Appendix A, we discuss a qualitative difference of the single-ion anisotropy and an exchange anisotropy from the viewpoint of ESR shifts.

II. FRAMEWORK

Here, we briefly review the perturbation theory of the ESR shift. ESR experiments measure an absorption of an electromagnetic wave by electron spins, where a microwave is typically applied. From the absorption spectrum, we are able to extract information on dynamics of electron spins. Within the linear response theory, the ESR spectrum $I(\omega) \propto \omega\chi''_{+-}(\omega,q)$ is written in terms of the retarded Green's function

$$\chi''_{+-}(\omega,q=0) = \mathrm{Im}\left[i \int_0^\infty dt\, e^{i\omega t} \langle [S^+(t), S^-(0)] \rangle \right]. \quad (2)$$

Here, $S^\pm = S^x \pm i S^y$ denote transverse components of the total spin $\boldsymbol{S} = \sum_j \boldsymbol{S}_j$, which is the generator of the global SU(2) symmetry. Thus, if the whole Hamiltonian preserves the SU(2) symmetry in the spin space, Eq. (2) is trivially constant. In the presence of the magnetic field, the symmetry of the Hamiltonian is lowered to U(1) at most. If spin-spin interactions preserve the SU(2) symmetry, Eq. (2) is still simple despite the presence of interactions

$$\chi''_{+-}(\omega,q=0) = 2\pi \langle S^z \rangle \delta(\omega - H). \quad (3)$$

The resonance frequency ω_r equals to the paramagnetic one $\omega_r = H$ at any temperature.

If spin-spin interactions do not preserve the SU(2) symmetry, the above discussion breaks down and the resonance frequency is shifted from the paramagnetic one. Let us assume that the Hamiltonian is composed of the three terms

$$\mathcal{H} = \mathcal{H}_0 + \mathcal{H}_Z + \mathcal{H}', \quad (4)$$

where $\mathcal{H}_0$ represents SU(2)-symmetric interactions, $\mathcal{H}_Z$ is the Zeeman term, and $\mathcal{H}'$ represents anisotropic interactions. The model (1) falls into the form of Eq. (4). If the anisotropic interaction is weak, we are able to consider a perturbative expansion of the resonance frequency in the anisotropy $\mathcal{H}'$.

The first-order perturbative expansion of the resonance frequency was proposed first by Kanamori and Tachiki[15] and later applied to quantum spin systems by Nagata and Tazuke.[10,16,17] Reference 18 derived the ESR shift $\delta\omega = \omega_r - H$ from equal-time correlations at the lowest order in a general formalism

$$\delta\omega = -\frac{\langle [[\mathcal{H}', S^+], S^-] \rangle_0}{2\langle S^z \rangle_0} + \cdots. \quad (5)$$

The average $\langle \ldots \rangle_0$ is taken with respect to the unperturbed Hamiltonian $\mathcal{H}^{(0)}$:

$$\mathcal{H}^{(0)} = \mathcal{H}_0 + \mathcal{H}_Z. \quad (6)$$

While we thus far treated the ESR spectrum as a function of the frequency ω with a fixed H in the above discussions, this is often not the case in actual ESR experiments. The ESR spectrum is usually obtained as a function of H with a fixed ω. In this case, the ESR shift is defined as

$$\delta H = H_r - \omega/g_e\mu_B. \quad (7)$$

H_r is the resonance field. Note that the g factor used in (7) is determined at the high-temperature limit. By definition, (7) approaches zero as $T \to +\infty$. At a low temperature $T \lesssim J$, it generally holds that $\delta H \neq 0$. According to Refs. 8 and 9, within the first-order accuracy, the ESR shift (7) satisfies

$$g_e\mu_B\delta H = \frac{\langle [[\mathcal{H}', S^+], S^-] \rangle_0}{2\langle S^z \rangle_0}. \quad (8)$$

We should emphasize that Eq. (8) is equivalent to (5). Therefore, as long as we are concerned with the first-order perturbation theory around (6), it does not matter whether we change ω or H.

We apply the formula (5) to our model (1), namely,

$$\mathcal{H}^{(0)} = J \sum_j \boldsymbol{S}_j \cdot \boldsymbol{S}_{j+1} - \sum_j \boldsymbol{H} \cdot \boldsymbol{S}_j, \quad (9)$$

$$\mathcal{H}' = D \sum_j \left(S_j^c\right)^2 + E \sum_j \left[\left(S_j^a\right)^2 - \left(S_j^b\right)^2\right]. \quad (10)$$

The ESR shift (5) is, in this case, given by

$$\delta\omega = f_D(\boldsymbol{z}) Y_D(T,H), \quad (11)$$

$$f_D(\boldsymbol{z}) = D\left(1 - 3{z_c}^2\right) - 3E\left({z_a}^2 - {z_b}^2\right), \quad (12)$$

$$Y_D(T,H) = \frac{1}{2\langle S^z \rangle_0} \sum_j \left[3\left\langle \left(S_j^z\right)^2 \right\rangle_0 - 2\right]. \quad (13)$$

The unit vector $\boldsymbol{z} \equiv \boldsymbol{H}/H$ is parallel to the magnetic field. $\boldsymbol{z}$ is represented as $\boldsymbol{z} = (z_a, z_b, z_c)$ in the principal (a,b,c) coordinate in (1). $f_D(\boldsymbol{z})$ is a constant (independent of T and H) if the orientation of the magnetic field is fixed. For simplicity, we hereafter set $\boldsymbol{H} = H\hat{z}$ where $\hat{z}$ is the unit vector along the c axis, that is, $\hat{z} = (0,0,1)$ in the principal axis coordinate. We call $Y_D(T,H)$ as a normalized ESR shift. The normalized ESR shift is useful for our purpose because it can be applied to systems with any value of D and E.

III. QMC RESULTS

We numerically evaluate the normalized ESR shift (13) from quantum Monte Carlo (QMC) calculations. The QMC results of the H dependence of $Y_D(T,H)$ are shown in Fig. 1. We find several characteristics from Fig. 1. (i) The normalized shift is approximately proportional to H in the ranges $0 < H < H_{c1}$ and $H_{c1} < H < H_{c2}$. The slope $\partial_H Y_D(T,H)$ is negative in the former and positive in the latter range. (ii) The normalized shift has a minimum around $H = H_{c1}$. The field which gives the minimum increases as the temperature increases. (iii) The normalized shift becomes zero at a certain value of H because $Y_D(T, H=0) = 0$ and $\partial_H Y_D(T,H)|_{H=0} < 0$ hold at $H = 0$ and the saturating value $Y_D(T, H > H_{c2})$ is positive. Note that the field dependence in Fig. 1 is qualitatively different from that of the $S = \frac{1}{2}$ HAF two-leg ladder systems.[19] In $S = \frac{1}{2}$ HAF two-leg ladder systems, we fail to find the change of the sign of the ESR shift. Namely, the normalized shift is nonzero from the infinitely weak field to the saturation field (see Fig. 1 in Ref. 19). The above three features suggest that the magnetic field dependence of the normalized ESR shift

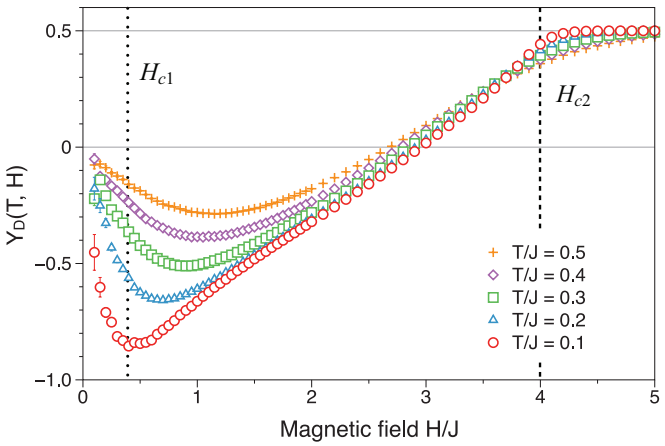

FIG. 1. (Color online) Quantum Monte Carlo results of the normalized ESR shift (13) induced by the single-ion anisotropy (10) for temperatures $T/J = 0.1$–0.5. The system size is $L = 40$ sites. The lower critical field $H_{c1} = 0.41J$ and the upper critical field $H_{c2} = 4J$ are guided by the dotted and the dashed lines, respectively. There is an extremum around $H = H_{c1} + T$. This nonmonotonic behavior of the ESR shift is understood by the finite-temperature crossover.

reflects the finite-temperature crossover. In the following, we analyze the normalized shift (13) in the gapped, lower critical, and upper critical regions.

IV. LOW-FIELD GAPPED PHASE

A. Effective field theory

First, we review the zero-field case, then we will extend the argument to the low-field case. The unperturbed model (6) in the absence of the magnetic field

$$\mathcal{H}_0 = J \sum_j \boldsymbol{S}_j \cdot \boldsymbol{S}_{j+1} \tag{14}$$

has an excitation gap $\Delta_0 = 0.41J$,[20] which is called as the Haldane gap. Haldane proposed that HAF chains with an integer quantum spin number S have an excitation gap Δ_0 based on a semiclassical field theory, the O(3) nonlinear sigma model (NLSM).[21,22] The O(3) NLSM has a Lagrangian

$$\mathcal{L} = \frac{1}{2g}\partial_\mu \boldsymbol{n} \cdot \partial^\mu \boldsymbol{n} + \frac{\Theta}{4\pi}\boldsymbol{n} \cdot \partial_t \boldsymbol{n} \times \partial_x \boldsymbol{n}. \tag{15}$$

The contraction $\partial_\mu \boldsymbol{n} \cdot \partial^\mu \boldsymbol{n} = (\partial_t \boldsymbol{n})^2 - (\partial_x \boldsymbol{n})^2$ was taken. For simplicity, we put the spin-wave velocity to unity. The field $\boldsymbol{n}(t,x)$ represents an antiferromagnetic order:

$$\boldsymbol{S}_x \sim \sqrt{S(S+1)}(-1)^x \boldsymbol{n}(x) + \boldsymbol{L}(x). \tag{16}$$

The uniform component $\boldsymbol{L} = \boldsymbol{n} \times \partial_t \boldsymbol{n}/g$ is quadratic in $\boldsymbol{n}$. The coupling constant $\Theta = 2\pi S$ is equal to 0 or π mod 2π.

The O(3) NLSM is integrable when $\Theta \equiv 0, \pi \pmod{2\pi}$. In the case $\Theta \equiv \pi$, the O(3) NLSM is critical.[23] On the other hand, in the case $\Theta \equiv 0$ of our interest, the O(3) NLSM has massive triplet particles, which are called magnons, as the lowest excitations. The triplet magnons are created by $n^a(t,x) \propto (-1)^x S^a(t,x)$ $(a = x,y,z)$. Thus, the field S^a satisfies the relation

$$(-1)^x \langle 0|S^a(t,x)|\theta_1,a_1\rangle = \delta_{aa_1}\sqrt{Z}e^{ix^\mu p_\mu}. \tag{17}$$

$|0\rangle$ is the ground state, $|\theta_1,a_1\rangle$ is a one-magnon state with the rapidity θ_1 and the index $a_1 = x,y,z$, and Z is the renormalization factor which will be discussed later. The O(3) NLSM is Lorentz invariant, and the triplet excitations obey a dispersion relation $p_0 = \sqrt{{\Delta_0}^2 + {p_1}^2}$ parametrized by a single parameter θ:

$$p_0 = \Delta_0 \cosh\theta, \quad p_1 = \Delta_0 \sinh\theta. \tag{18}$$

This parameter θ is called a rapidity, which uniquely determines the energy p_0 and the momentum p_1 of magnons. Therefore, the one-magnon state $|\theta_1,a_1\rangle$ is fully characterized by the rapidity θ_1 and the index a_1. We normalize the state $|\theta,a\rangle$ by

$$\langle\theta_1,a_1|\theta_2,a_2\rangle = 4\pi\delta_{a_1a_2}\delta(\theta_1 - \theta_2). \tag{19}$$

n-magnon states $|\theta_1,a_1;\ldots;\theta_n,a_n\rangle$ are specified by a set of rapidities $\{\theta_1,\ldots,\theta_n\}$ and indices $\{a_1,\ldots,a_n\}$. They are normalized as follows:

$$\begin{aligned}&\langle\theta_1,a_1;\ldots;\theta_n,a_n|\theta'_1,a'_1;\ldots;\theta'_n,a'_m\rangle \\ &\quad = \delta_{nm}(4\pi)^n \prod_{l=1}^{n} \delta_{a_la'_l}\delta(\theta_l - \theta'_l).\end{aligned} \tag{20}$$

A matrix element

$$F_{\mathcal{O}}(\theta_1,a_1;\ldots;\theta_n,a_n) = \langle 0|\mathcal{O}(0)|\theta_1,a_1;\ldots;\theta_n,a_n\rangle \tag{21}$$

is called an n-magnon form factor of a local operator $\mathcal{O}(t,x)$. Here, $\mathcal{O}(0)$ is an abbreviation of $\mathcal{O}(0,0)$. A Lorentz boost of the O(3) NLSM alters (21) to

$$\begin{aligned}&\langle 0|\mathcal{O}(t,x)|\theta_1,a_1;\ldots;\theta_n,a_n\rangle \\ &\quad = F_{\mathcal{O}}(\theta_1,a_1;\ldots;\theta_n,a_n)e^{i(tP_0 - xP_1)},\end{aligned} \tag{22}$$

where P_0 and P_1 denote the total energy and momentum:

$$P_0 = \sum_{m=1}^{n} \Delta_0 \cosh\theta_m, \quad P_1 = \sum_{m=1}^{n} \Delta_0 \sinh\theta_m. \tag{23}$$

For example, the relation (17) is equivalent to the one-magnon form factor of S^a at the origin

$$F_{S^a}(\theta_1,a_1) = (-1)^r\sqrt{Z}\delta_{a,a_1}. \tag{24}$$

The relation (17) connects the low-energy effective field theory and the physical operator $S^a(t,x)$ in the original spin model. The renormalization factor $\sqrt{Z}$ inevitably depends on short-distance, nonuniversal physics and can not be determined within the effective field theory. Z is determined only by numerical calculations. $Z \approx 1.26$ is concluded from density matrix renormalization group calculations.[24,25] It is emphasized that Eq. (24) should *not* be interpreted as an identity between the physical spin operator S^a and a creation operator of magnons. The spin operator S^a also has nonvanishing higher-order form factors. Thus, the form factor of the powers of S^a is not solely determined by the one-magnon form factor (24), even in the leading order.

Let us consider the traceless symmetric tensor

$$\Sigma^{ab} \equiv S^a S^b - \tfrac{2}{3}\delta_{ab}. \tag{25}$$

Σ^{ab} has a two-magnon form factor

$$F_{\Sigma^{ab}}(\theta_1,a_1;\theta_2,a_2) = -iZ_2\delta_{ab}\delta_{a_1a_2}(3\delta_{aa_1}-1)\psi_2(\theta_1-\theta_2). \tag{26}$$

In the case of O(N) NLSM,[26] $\psi_2(\theta)$ is given by an integral

$$\psi_2(\theta) = \sinh\left(\frac{\theta}{2}\right)\exp\left[\int_0^\infty \frac{dx}{x}K_N(x)\frac{\cosh[(\pi+i\theta)x]-1}{\sinh(\pi x)}\right], \tag{27}$$

$$K_N(x) = \frac{e^{-\pi x}+e^{-2\pi x/(N-2)}}{1+e^{-\pi x}}. \tag{28}$$

We performed the integral and derived an explicit form of $\psi_2(\theta)$ for the $N=3$ case in our preceding paper[13]:

$$\psi_2(\theta) = \frac{i}{2}(\theta-\pi i)\tanh\left(\frac{\theta}{2}\right). \tag{29}$$

The two-magnon form factor (26) is now determined except for the nonuniversal factor Z_2. We emphasize that Z_2 is an independent parameter from Z. We have determined $Z_2 \approx 0.24$ by comparing the NLSM prediction with the correlation function of $(S^a)^2$ obtained numerically using the infinite time evolving block decimation method.[13]

The basis $\{|\theta_1,a_1;\ldots;\theta_n,a_n\rangle\}$ with $n=0,1,2,\ldots$ is complete and orthonormal. The identity $\hat{1}$ reads as

$$\hat{1} = |0\rangle\langle 0| + \sum_{n=1}^\infty \frac{1}{n!}\sum_{a_1\ldots a_n}\int_{-\infty}^\infty \frac{d\theta_1\ldots d\theta_n}{(4\pi)^n} \times |\theta_1,a_1;\ldots;\theta_n,a_n\rangle\langle\theta_1,a_1;\ldots;\theta_n,a_n|. \tag{30}$$

We note an important relation of form factors: the crossing relation. In subsequent sections, we will encounter matrix elements such as $\langle\theta_2,a_2|\mathcal{O}(0)|\theta_1,a_1\rangle$. The crossing relation allows one to relate this matrix element to form factors

$$\begin{aligned}\langle\theta_2,a_2|\mathcal{O}(0)|\theta_1,a_1\rangle &= \langle 0|\mathcal{O}(0)|\theta_1,a_1;\theta_2-\pi i,\bar{a_2}\rangle \\ &= F_{\mathcal{O}}(\theta_1,a_1;\theta_2-\pi i,\bar{a_2}).\end{aligned} \tag{31}$$

The index $\bar{a}$ represents an index of an antimagnon conjugate to the magnon with the index a. If we employ the labeling $a=x,y,z$, then $\bar{a}=a$ holds. If, on the other hand, we employ a labeling $a=+,0,-$, namely $(n^+,n^0,n^-)=[(n^x+in^y)/\sqrt{2},n^z,(n^x-in^y)/\sqrt{2}]$, we have $\bar{+}=-$, $\bar{0}=0$, and $\bar{-}=+$.

Under a weak magnetic field $H<\Delta_0$, the unperturbed system (9) still has a finite gap Δ_0-H. Here, we have to replace the dispersion relation (18) to

$$p_0 = \Delta_0\cosh\theta - aH, \quad p_1 = \Delta_0\sinh\theta, \tag{32}$$

where $a=0,+,-$. Namely, the triplet degeneracy is lifted by the Zeeman splitting term. If the magnetic field is very weak $H \ll \Delta_0$, then we may use the form factors evaluated for the $H=0$ case at the lowest order of H. For this purpose, in the following, we use the labeling $a=+,0,-$ of magnons, which corresponds to energy eigenstates under the magnetic field.

B. ESR shift

In the limit $H,T\to 0$, the density of magnons becomes low. It should be reasonable in this dilute limit that we ignore contributions of multimagnon states to thermodynamic quantities, for instance, the magnetization and the normalized shift (13). We multiply a projection operator

$$P_1 = \sum_{a=0,+,-}\int_{-\infty}^\infty \frac{d\theta}{4\pi}|\theta,a\rangle\langle\theta,a|$$

to an operator $\mathcal{O}$ so that the multimagnon contributions to the average $\langle\mathcal{O}\rangle$ are projected out. Let us consider $\mathcal{O}=\Sigma^{00}(0,x)$. Using the crossing relation (31) and the two-magnon form factor (26), we obtain

$$\begin{aligned}&P_1\Sigma^{00}(0,x)P_1 \\ &= -iZ_2\int_{-\infty}^\infty \frac{d\theta\,d\theta'}{(4\pi)^2}\psi_2(\theta'-\theta+\pi i)e^{ix[P_1(\theta')-P_1(\theta)]} \\ &\quad\times(2|\theta,0\rangle\langle\theta,0| - |\theta,+\rangle\langle\theta',+|-|\theta,-\rangle\langle\theta',-|).\end{aligned} \tag{33}$$

Thus, in the dilute limit, the numerator $\sum_j[3\langle(S_j^z)^2\rangle_0-2]$ of the normalized shift (13) is approximated as follows:

$$\begin{aligned}&\sum_j\left[3\left\langle\left(S_j^z\right)^2\right\rangle_0-2\right] \\ &= 3\int dx\,\langle\Sigma^{00}(0,x)\rangle_0 \\ &\sim -6Z_2\int_{-\infty}^\infty \frac{v\,d\theta}{4\pi E(\theta)}e^{-E(\theta)/T}\sinh^2\left(\frac{H}{2T}\right).\end{aligned} \tag{34}$$

Here, $E(\theta)=\Delta_0\cosh\theta$ is the zero-field dispersion. Similarly, the magnetization is given by

$$\langle S^z\rangle_0 \sim 2\sinh\left(\frac{H}{T}\right)\int_{-\infty}^\infty\frac{d\theta}{4\pi}e^{-E(\theta)/T}. \tag{35}$$

From (34) and (35), the normalized shift in the dilute limit reads as

$$Y_D(T,H) = -\frac{3Z_2}{4}\tanh\left(\frac{H}{2T}\right)\frac{\int_{-\infty}^\infty\frac{v\,d\theta}{4\pi E(\theta)}e^{-E(\theta)/T}}{\int_{-\infty}^\infty\frac{d\theta}{4\pi}e^{-E(\theta)/T}}. \tag{36}$$

Equation (36) correctly reproduces the features of the normalized shift $Y_D(T,H)\propto H$ and $\partial_H Y_D(T,H)<0$ in the limit $H\to 0$. However, (36) can not explain the upturn of the normalized shift around $H=H_{c1}$. In order to extend (36) to the region $H\sim H_{c1}$, we must take into account multimagnon states.

V. NEAR LOWER CRITICAL FIELD

A. Effective field theory

At $H=\Delta_0$, the lowest magnon band specified by the index $a=+$ touches the ground state. The point $H_{c1}\equiv\Delta_0$ corresponds to a quantum critical point. Above H_{c1}, gapless excitations exist. Thus, $H=H_{c1}$ separates the low-field gapped phase (called as the Haldane phase) and the high-field gapless phase (the field-induced critical phase). We call H_{c1} the lower critical field. The quantum phase transition occurs only at $T=0$. Nevertheless, at finite temperatures, in a range of magnetic field $H-H_{c1}\leqslant T$, which is called as "quantum critical region," properties of the system reflect the nature of the quantum critical point.[27]

It is known that a free-fermion theory describes low-energy behavior of $S=1$ HAF chain in the quantum critical

region.[1,28–31] The free fermion has a dispersion relation

$$E(k) = \frac{k^2}{2\Delta_0} - \mu. \tag{37}$$

The chemical potential is $\mu = H - H_{c1}$. As the chemical potential of the free fermion increases, the number of the free fermion also increases. In terms of spin systems, the number of the free fermion is identical to the magnetization density $m_+(T,H) \equiv \langle S^z\rangle_0/L$:

$$\begin{aligned} m_+(T,H) &= \sqrt{\frac{\Delta_0}{2\pi^2}}\int_0^\infty d\epsilon\, D(\epsilon) f(\epsilon-\mu) \\ &= -\sqrt{\frac{T\Delta_0}{2\pi}}\,\mathrm{Li}_{1/2}(-e^{\mu/T}). \end{aligned} \tag{38}$$

L is the length of the spin chain, $D(\epsilon) = \epsilon^{-1/2}$ is the density of states, and $f(\xi) = (e^{\xi/T}+1)^{-1}$ is the Fermi distribution function. In the second line, the integral is performed explicitly, with the result given in terms of the polylogarithm function

$$\mathrm{Li}_n(x) = \sum_{m=1}^{\infty}\frac{x^m}{m^n}. \tag{39}$$

Above the quantum critical region $H \gtrsim H_{c1}$, a gapless excitation with a linear dispersion $E(k) \sim k$ dominates the low-temperature physics of the $S = 1$ HAF chain. The excitation is identified with the Tomonaga-Luttinger (TL) liquid.[2,32] We do not go into detail on the TL liquid in the field-induced critical phase.

B. ESR shift

In the previous section, we formulated the O(3) NLSM with the multimagnon states $|\theta_1,a_1;\ldots;\theta_n,a_n\rangle$. Instead of these multimagnon states, we may consider creation and annihilation operators of magnons, which we denote $Z_a(\theta)$ and $Z_a^\dagger(\theta)$, respectively. Using them, we can create a one-magnon state $|\theta,a\rangle$ and its conjugate

$$|\theta,a\rangle = Z_a^\dagger(\theta)|0\rangle, \quad \langle\theta,a| = \langle 0|Z_a(\theta). \tag{40}$$

Similarly, the n-magnon state and its conjugate are given by

$$\begin{aligned} |\theta_1,a_1;\ldots;\theta_n,a_n\rangle &= Z_{a_1}^\dagger(\theta_1)\ldots Z_{a_n}^\dagger(\theta_n)|0\rangle, \\ \langle\theta_1,a_1;\ldots;\theta_n,a_n| &= \langle 0|Z_{a_n}(\theta_n)\ldots Z_{a_1}(\theta_1). \end{aligned}$$

These $Z_a(\theta)$ and $Z_a^\dagger(\theta)$ are called Faddeev-Zamolodchikov (FZ) operators and satisfy the following algebra:

$$Z_{a_1}(\theta_1)Z_{a_2}(\theta_2) = S_{a_1a_2}^{b_1b_2}(\theta_1-\theta_2)Z_{b_2}(\theta_2)Z_{b_1}(\theta_1), \tag{41}$$

$$Z_{a_1}^\dagger(\theta_1)Z_{a_2}^\dagger(\theta_2) = S_{a_1a_2}^{b_1b_2}(\theta_1-\theta_2)Z_{b_2}^\dagger(\theta_2)Z_{b_1}^\dagger(\theta_1), \tag{42}$$

$$\begin{aligned} Z_{a_1}(\theta_1)Z_{a_2}^\dagger(\theta_2) &= 4\pi\delta_{a_1a_2}\delta(\theta_1-\theta_2) \\ &\quad + S_{a_2b_1}^{b_2a_1}(\theta_1-\theta_2)Z_{b_2}^\dagger(\theta_2)Z_{b_1}(\theta_1). \end{aligned} \tag{43}$$

The factor $S_{ab}^{cd}(\theta)$ is an S matrix. The S matrix possesses information of two-magnon scatterings. If the magnon created by $Z_a^\dagger(\theta)$ were a free boson (a free fermion), the S matrix would simply be $S_{ab}^{cd}(\theta) = \delta_{ad}\delta_{bc}$ [$S_{ab}^{cd}(\theta) = -\delta_{ad}\delta_{bc}$]. In reality, the magnon is neither free boson nor fermion. Thus, the S matrix is a nontrivial function of the rapidity. Fortunately, the S matrix of the O(3) NLSM is exactly known:

$$S_{ab}^{cd}(\theta) = \delta_{ab}\delta_{cd}\sigma_1(\theta) + \delta_{ac}\delta_{bd}\sigma_2(\theta) + \delta_{ad}\delta_{bc}\sigma_3(\theta). \tag{44}$$

$\sigma_i(\theta)$'s ($i = 1,2,3$) are

$$\sigma_1(\theta) = \frac{2\pi i\theta}{(\theta+\pi i)(\theta-2\pi i)}, \tag{45}$$

$$\sigma_2(\theta) = \frac{\theta(\theta-\pi i)}{(\theta+\pi i)(\theta-2\pi i)}, \tag{46}$$

$$\sigma_3(\theta) = \frac{2\pi i(\pi i-\theta)}{(\theta+\pi i)(\theta-2\pi i)}. \tag{47}$$

As well as the set of multimagnon states $\{|\theta_1,a_1;\ldots;\theta_n,a_n\rangle\}$, a set of FZ operators $\{Z_a(\theta),Z_b^\dagger(\theta')\}$ is complete. In other words, we can expand the arbitrary operator $\mathcal{O}(t,x)$ in the power of FZ operators. For instance, $\int dx\ \Sigma^{aa}(0,x)$ is expanded as

$$\begin{aligned} &\int dx\ \Sigma^{aa}(0,x) \\ &\quad = \frac{Z_2}{2}\int_{-\infty}^{\infty}\frac{v\,d\theta}{4\pi E(\theta)}[2Z_0^\dagger(\theta)Z_0(\theta) - Z_+^\dagger(\theta)Z_+(\theta) \\ &\qquad - Z_-^\dagger(\theta)Z_-(\theta)] + (\text{higher-order terms}). \end{aligned} \tag{48}$$

The omitted higher-order terms contain, for instance, a quartic term $Z_{a_1}^\dagger(\theta_1)Z_{a_2}(\theta_2)Z_{a_3}^\dagger(\theta_3)Z_{a_4}(\theta_4)$. The projection (33) corresponds to an approximation which drops the higher-order terms of (48) out. To improve the result (36), we need to accurately evaluate the higher-order terms of the expansion (48).

At low temperatures and around the lower critical field, we can focus on the low-energy limit of NLSM. Here, the S matrix of the O(3) NLSM actually simplifies as

$$S_{ab}^{cd}(\theta) \to -\delta_{ad}\delta_{bc}, \tag{49}$$

which is nothing but the S matrix of free fermions. This implies that, in this limit, we can replace the FZ operators by the fermion creation and annihilation operators as

$$Z_a(\theta) \sim \sqrt{\frac{2E(\theta)}{v}}\,c_a(k), \quad Z_a^\dagger(\theta) \sim \sqrt{\frac{2E(\theta)}{v}}\,c_a^\dagger(k), \tag{50}$$

with $k = \Delta_0\sinh\theta$. The rule (50) correctly reproduces the anticommutation relations

$$\{c_a(k),c_{a'}(k')\} = 0, \tag{51}$$

$$\{c_a^\dagger(k),c_{a'}^\dagger(k')\} = 0, \tag{52}$$

$$\{c_a(k),c_{a'}^\dagger(k')\} = 2\pi\delta_{aa'}\delta(k-k') \tag{53}$$

from Eqs. (41), (42), and (43). This fermion has a dispersion $E_a(k) = \sqrt{{\Delta_0}^2+k^2} - aH$ ($a = 0,+,-$), and indeed corresponds exactly to the free-fermion effective theory discussed in Sec. V A. In other words, the free-fermion effective theory for the quantum critical region is now derived systematically as a low-energy limit of the O(3) NLSM under an applied field.

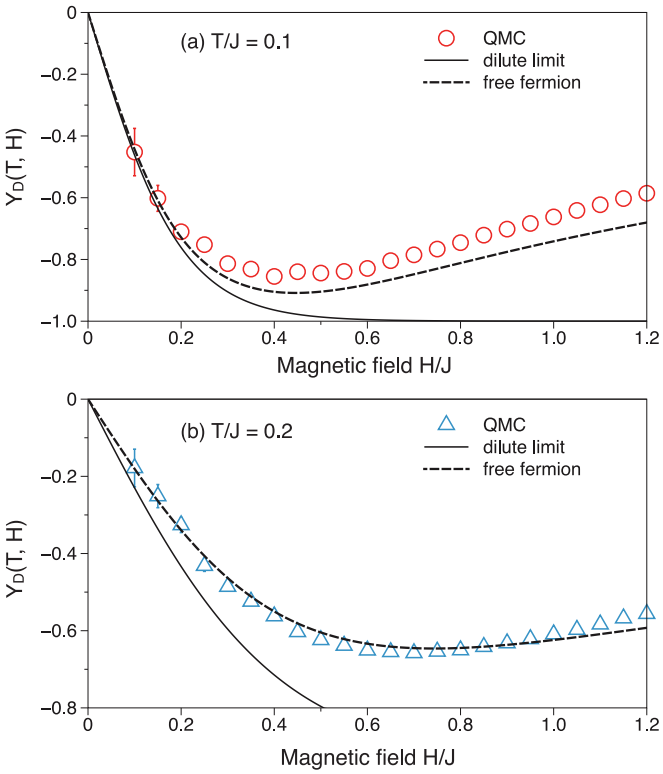

FIG. 2. (Color online) Comparisons of QMC and analytic results at (a) $T/J = 0.1$ and at (b) $T/J = 0.2$. Open symbols (circles and triangles) represent QMC data. The solid curves denote the normalized shift in the dilute limit (36). The dashed curves correspond to (54).

The replacement (50) enables us to compute the normalized shift explicitly:

$$Y_D(T,H) = \frac{3Z_2}{2m(T,H)} \int_{-\infty}^{\infty} \frac{v\,dk}{4\pi E_0(k)} [2f_0(k) - f_+(k) - f_-(k)]. \tag{54}$$

$f_a(k) = (e^{(\sqrt{\Delta_0^2+k^2}-aH)/T} + 1)^{-1}$ is the Fermi distribution function and $m(T,H)$ is the magnetization

$$m(T,H) = \int_{-\infty}^{\infty} \frac{dk}{2\pi} [f_+(k) - f_-(k)]. \tag{55}$$

The analytic result (54) is compared with the QMC results at $T = 0.1J$ and $0.2J$ in Fig. 2. The free-fermion representation (54) reproduces the minimum of the normalized ESR shift and, furthermore, agrees quantitatively with the QMC data. We stress that the systematic derivation based on the exact form factors of the O(3) NLSM is necessary to obtain Eq. (54) correctly. In fact, it contains the nontrivial renormalization factor Z_2, which is independent of the standard renormalization factor Z. A naive application of the free-fermion effective theory would lead to a formula similar to Eq. (54) but with Z appearing in the place of Z_2. Clearly, it does not agree with the QMC result, demonstrating the importance of the form-factor approach.

VI. NEAR UPPER CRITICAL FIELD

A. Effective field theory

The field-induced critical phase ends at the upper critical field $H = H_{c2}$ where $H_{c2} = 4J$. Above the upper critical field, the spins are fully polarized, where the gap opens again and the low-energy excitation has a parabolic dispersion. Slightly below the upper critical field ($H_{c2} \ll H - H_{c2} < 0$), almost all spins are polarized. Here, we may neglect the $S_j^z = -1$ component antiparallel to the magnetic field because it costs huge amounts of energy. Thus, the $S = 1$ spin is effectively described by an $S = \frac{1}{2}$ spin:

$$S_j^z \sim \frac{1}{2}(1 + \sigma_j^z), \quad S_j^{\pm} \sim \frac{1}{\sqrt{2}}(-1)^j \sigma_j^{\pm}. \tag{56}$$

$(\sigma_j^x, \sigma_j^y, \sigma_j^z)$ are the Pauli matrices and $\sigma_j^{\pm} \equiv (\sigma_j^x \pm i\sigma_j^y)/2$. The unperturbed Hamiltonian (9) is transformed into an effective $S = \frac{1}{2}$ XXZ chain

$$\mathcal{H}^{(0)} \sim \frac{J}{2} \sum_j \left[-\left(\sigma_j^x \sigma_{j+1}^x + \sigma_j^y \sigma_{j+1}^y\right) + \frac{1}{2}\sigma_j^z \sigma_{j+1}^z \right] - \frac{h}{2} \sum_j \sigma_j^z. \tag{57}$$

This is effectively written in terms of a free fermion

$$\mathcal{H}^{(0)} \sim \int_{-\infty}^{\infty} \frac{dk}{2\pi} E(k) c^{\dagger}(k) c(k), \tag{58}$$

with a quadratic dispersion

$$E(k) = \frac{k^2}{2\mathfrak{m}} - \tilde{\mu}. \tag{59}$$

Here, $\mathfrak{m} = 1/2J$ and $\tilde{\mu} = H_{c2} - H$ are the mass of the fermion and the chemical potential that the fermion feels. Thus, the effective theories around the upper critical field field and the lower critical field are isomorphic, while the mass and the chemical potential of the fermions are different. It should be also noted that the free fermion in each theory represents a different object with respect to the original spin system.

B. ESR shift

Using the mapping (56), one can represent the normalized shift in the Pauli matrices

$$Y_D(T,H) = \frac{1}{2} - \frac{1 - \langle\sigma_j^z\rangle_0}{1 + \langle\sigma_j^z\rangle_0}. \tag{60}$$

Here, the average $\langle\ldots\rangle_0$ is taken by the Hamiltonian (57) of the effective $S = \frac{1}{2}$ XXZ chain. A free-fermion theory with the dynamical exponent $z = 2$ describes the low-energy physics near the upper critical field H_{c2}. Similarly to Eq. (38), the magnetization density $\langle\sigma_j^z\rangle_0$ is given by the polylogarithm function as

$$\langle\sigma_j^z\rangle_0 = 1 + 2\sqrt{\frac{T}{4\pi J}}\,\mathrm{Li}_{1/2}\left(-e^{(H_{c2}-H)/T}\right). \tag{61}$$

Substituting (61) into (60), we obtain the explicit representation of the normalized shift. We show the normalized ESR shift computed by the free-fermion theory in Fig. 3. In order to see the field dependence explicitly, we consider the $T = 0$

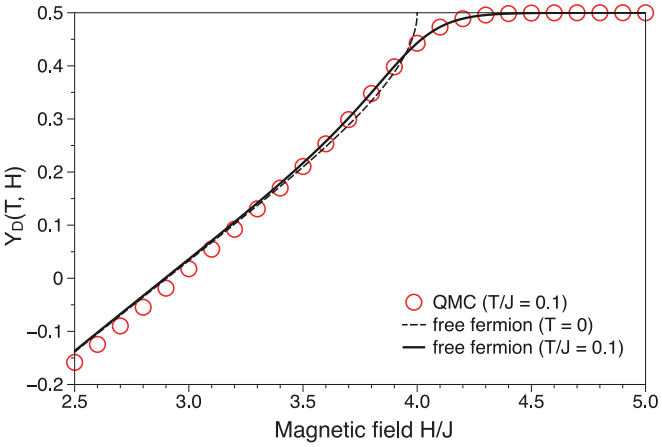

FIG. 3. (Color online) The open circles denote the QMC data obtained for 40-site chains at $T/J = 0.1$. The solid and dashed curves are derived from the free-fermion theory near H_{c2}. The former is $T > 0$ data and the latter is $T = 0$ data. The finite-temperature effect is irrelevant in the lower-field range $H \lesssim 3J$.

case. The magnetization shows a singular dependence on the magnetic field at $T = 0$:

$$\langle \sigma_j^z \rangle_0 = 1 - \frac{2}{\pi}\sqrt{H_{c2} - H} + \mathcal{O}(H_{c2} - H). \qquad (62)$$

The normalized shift at $T = 0$ is shown by the dashed curve in Fig. 3. The free-fermion theory (58) appears to work well in the entire region of Fig. 3 in the limit of $T \to 0$. However, the numerical result in Fig. 1 shows a non-negligible temperature dependence for $H \lesssim 3J$, while the free-fermion theory shows little temperature dependence. This corresponds to the breakdown of the present picture based on spin flips from the saturated state, in the lower magnetic field.

VII. NDMAP

We apply our theory of ESR shifts to an $S = 1$ HAF chain compound $Ni(C_5H_{14}N_2)_2N_3(PF_6)$ [abbreviated to NDMAP (Refs. 5,33–35)]. There are several $S = 1$ HAF chain compounds, for instance, $Ni(C_2H_8N_2)_2(NO_2)ClO_4$ [abbreviated to NENP (Ref. 36)], $Ni(C_9H_{24}N_4)(NO_2)ClO_4$ [abbreviated to NTENP (Ref. 37)], and $Ni(C_5H_{14}N_2)_2N_3(ClO_4)$ [abbreviated to NDMAZ (Ref. 38)]. Among these $S = 1$ HAF chain compounds, NDMAP is most suitable to our purpose because NENP has an effective staggered magnetic field $h\sum_j (-1)^j S_j^x$ and NTENP has a bond alternation $\delta \sum_j (-1)^j \boldsymbol{S}_j \cdot \boldsymbol{S}_{j+1}$. The staggered magnetization mixes the singlet ground state $|g\rangle$ and the triplet excited states $|e\rangle$: $\langle e|\sum_j (-1)^j S_j^x|g\rangle \neq 0$.[12] This mixing changes the selection rule of ESR. Such an interaction is uncovered by our theory. Although the bond alternation does not induce the mixing, when $H = 0$, NTENP has a different ground state from that of (9).[39] Recently, NTENP has been field theoretically analyzed by using a sine-Gordon model.[40] The compound NDMAZ has very similar crystal structure to NDMAP. In fact, our theory is applicable to NDMAZ. But, NDMAZ has stronger exchange interaction $J \approx 70.6$ K than NDMAP. The large J makes the experimental investigation of the field-induced critical phase difficult because of the large H_{c1}.

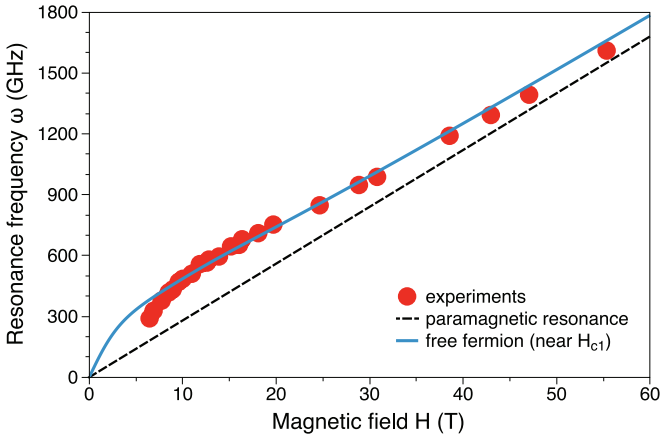

FIG. 4. (Color online) Comparison of the free-fermion theory (54) with the experimental data on NDMAP at a temperature $T = 0.05J$ (Ref. 5). The solid curve is the free-fermion result (54) near H_{c1} and the solid circles denote the experimental data. We used the parameters $J = 30.0$ K, $D/J = 0.25$, and $g_e = 2.10$. The magnetic field is applied along the c axis, which corresponds to $z_p = 1$, $z_q = z_r = 0$. The dashed curve is high-temperature paramagnetic resonance frequency $\omega = g_e\mu_B H$.

Parameters of NDMAP are estimated as follows[34]:

$$J \approx 30.0 \text{ K}, \quad D/J \approx 0.25. \qquad (63)$$

The parameter E is much smaller than D. Here, we consider the field orientation perpendicular to the easy plane $(z_p, z_q, z_r) = (1,0,0)$. Thus, the normalized shift is independent of the anisotropy E:

$$\omega_r = g_e\mu_B H - 2DY_D(T,H). \qquad (64)$$

The Landé g factor is $g_e = 2.11$.[5] We substitute the free-fermion theory near the lower critical field (54) into (64) and compare it with experimental data by Ref. 5 (Fig. 4). They show semiquantitative agreement. Our theory gives a concrete support to the estimation (63).

Note that there is a zero point $H = H_0(T)$ where the ESR shift vanishes,

$$Y_D(T, H_0(T)) = 0. \qquad (65)$$

In addition to the trivial solution $H_0 = 0$, at $T = 0.1J$, one can find a zero point $H_0 \sim 3J$ in Fig. 5. We show several cases $D/J = 0.1$, 0.2, and -0.1 with the fixed J. One will be able to experimentally observe the zero point $H = H_0$ if an $S = 1$ HAF chain compound with smaller $J \lesssim 15$ K is found. In general, the zero point $H_0(T)$ depends on the temperature T. The nontrivial solution $H_0(T)$ of (65) exists in a wide range of the temperature because $Y_D(T,H)$ is negative in $H \ll H_{c1}$ and positive in $H \sim H_{c2}$. In contrast, as we will discuss in the Appendix, for the exchange anisotropy

$$\mathcal{H}' = \sum_j \sum_{a=p,q,r} J'_a S_j^a S_{j+1}^a, \qquad (66)$$

we find that the ESR shift in the first order of the anisotropy does not change its sign in the entire range of H.

By measuring the zero-field excitation gaps, the symmetry of the Hamiltonian (4) can be identified experimentally. Let us

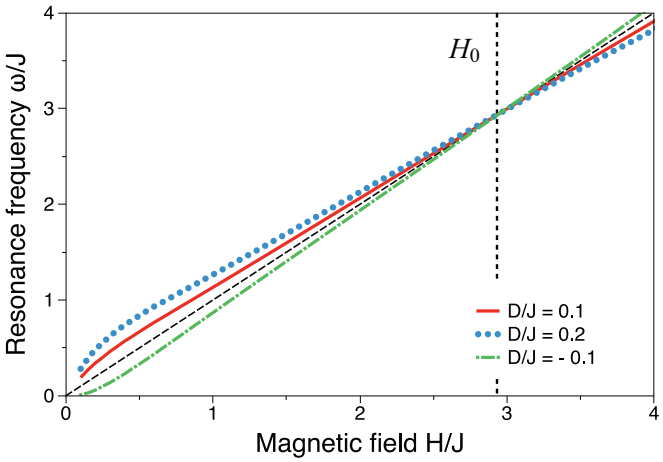

FIG. 5. (Color online) QMC data of the resonance frequency (64) at $T = 0.1J$. The g factor is set to $g_e\mu_B = 1$ for simplicity. The dashed line $\omega = H$ corresponds to the paramagnetic resonance frequency. Several cases $D/J = 0.1$, 0.2, and -0.1 are shown. Note that there is a zero point $H_0 \sim 3J$ where the shift (5) vanishes.

suppose that the Hamiltonian has a uniaxial, U(1) symmetry, broken from the rotational SU(2) symmetry. This is consistent with a presence of either the single-ion anisotropy (10) or the exchange anisotropy (66). It is usually difficult to distinguish these two kinds of anisotropic interactions because they often lead to qualitatively the same consequences in observables. However, the presence or absence of the zero point $H_0(T)$ of the shift at $T \sim H_{c1}$ is a clear signature which distinguishes the two cases. This may provide a new application of ESR, which possesses a high sensitivity to anisotropy unavailable in other types of measurements.

VIII. SUMMARY

We theoretically investigated the ESR shift caused by a weak single-ion anisotropy in the $S = 1$ HAF chain. We applied the Kanamori-Tachiki theory (5) to this system, and analyzed it both analytically and numerically. The formula (5) is factorized to $\delta\omega = f_D(z)Y_D(T,H)$, which is composed of the T, H-independent geometrical factor $f_D(z)$ and the T, H-dependent factor $Y_D(T,H)$. In this paper, we call $Y_D(T,H)$ as the normalized ESR shift because the factor $f_D(z)$ can be regarded as a constant if we fix the field orientation z. In contrast, the normalized shift $Y_D(T,H)$ does not depend on the field orientation. Thus, this factorization allows the general analysis of the ESR shift without specifying the parameters D and E.

Quantum Monte Carlo calculations revealed nonmonotonic magnetic field dependence of the normalized shift $Y_D(T,H)$. The field dependence reflects the finite-temperature crossover of the $S = 1$ HAF chain, the low-field gapped phase ($H < H_{c1}$), the field-induced critical phase ($H_{c1} < H < H_{c2}$), and the fully polarized phase ($H_{c2} < H$). We employed several effective field theories to explain the field dependence of $Y_D(T,H)$ in each phase. We used the exact form factors to compute $Y_D(T,H)$ in the dilute limit $H,T \to 0$. We extend the result in the low-field limit to the finite-field region $H \sim H_{c1}$ by replacing the FZ operators of the lowest excitations to the fermionic creation and annihilation operators. This replacement is reasonable in $H \lesssim H_{c1}$ and it works quite well (Fig. 2). Above H_{c1}, the system is regarded as the TL liquid. Although we did not go into detail of the ESR shift of the TL liquid in the field-induced critical phase, it can be extracted from the analyses around H_{c1} and H_{c2}. Near the upper critical field H_{c2}, the free-fermion analysis is again effective (Fig. 3).

Our analysis is found to agree semiquantitatively with the experimental data of NDMAP in Ref. 5. Our theory correctly reproduces the approaching of the resonance frequency to the paramagnetic resonance frequency $\omega = g_e\mu_B H$. Furthermore, we predicted the existence of the special value H_0 of the magnetic field where the ESR shift vanishes $\delta\omega = 0$. Such a sign change is absent in the case of an exchange anisotropy.

As a final remark, we point out that one can experimentally determine the field dependence of nontrivial quantities such as $\langle (S^z_j)^2 \rangle$ and $\langle S^z_j S^z_{j+1} \rangle$ from the ESR shifts (13) and (A3). The quantity $\langle (S^z_j)^2 \rangle$ is a nontrivial function of H and T: in an isotropic chain, it takes $\frac{2}{3}$ at $H = 0$, decreases first as H is increased, but increases asymptotically towards the saturation value 1 in the limit $H \to +\infty$. This nonmonotonic dependence is reflected in the shift (13).

ACKNOWLEDGMENTS

This work is supported by a Grant-in-Aid for Scientific Research No. 21540381 (M.O.) and the Global COE Program "The Physical Sciences Frontier" (S.C.F.) from MEXT, Japan. We thank the ALPS project for providing the quantum Monte Carlo code.[41]

APPENDIX: EXCHANGE ANISOTROPY

We have so far considered the single-ion anisotropy as a resource of anisotropic interactions. In this appendix, we treat a perturbative exchange anisotropy instead of the single-ion anisotropy (10). The ESR shift caused by the exchange anisotropy (66) is also factorized just like (11):

$$\delta\omega = f_{J'}(z)Y_{J'}(T,H), \tag{A1}$$

$$f_{J'}(z) = \sum_{a=p,q,r} J'_a\left(1 - 3z_a{}^2\right), \tag{A2}$$

$$Y_{J'}(T,H) = \frac{1}{2\langle S^z\rangle_0} \sum_j \sum_{a=x,y,z} (3\delta_{az} - 1)\left\langle S^a_j S^a_{j+1}\right\rangle_0. \tag{A3}$$

We compute the normalized shift (A3) by QMC in the same manner as (13). Figure 6 shows QMC results of the normalized shift (A3) at temperatures $T/J = 0.1$–0.5. The normalized shift $Y_{J'}(T,H)$ behaves similarly to $Y_D(T,H)$ in a region where $T < 0.3J$ and $H < J$ hold. On the other hand, in a higher-field region $H > J$, the normalized shift quickly saturates to 1.

First, we consider the zero-field case. The effective field theory O(3) NLSM works well at $H = 0$. When we move on to the continuum limit, we approximate the product $S^a_j S^a_{j+1}$ by the composite operator $[S^a(x)]^2$:

$$S^a_j S^a_{j+1} \sim -C[S^a(x)]^2. \tag{A4}$$

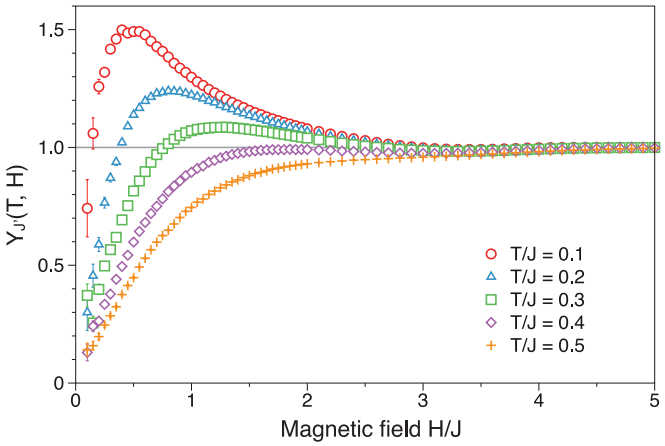

FIG. 6. (Color online) Quantum Monte Carlo results of the normalized ESR shift (A3) induced by the exchange anisotropy (66) for temperatures $T/J = 0.1$–0.5. The system size is $L = 40$ sites. The maximum around $H = H_{c1} + T$ is also found in this case. The field dependence of $Y_{J'}(T,H)$ in a lower field region $H < J$ at low temperatures $T < 0.3J$ looks similar to that of $Y_D(T,H)$ except the overall sign $Y_{J'}(T,H) \propto -Y_D(T,H)$. In a relatively higher temperature $T > 0.4J$, the nonmonotonic behavior of the normalized shift vanishes.

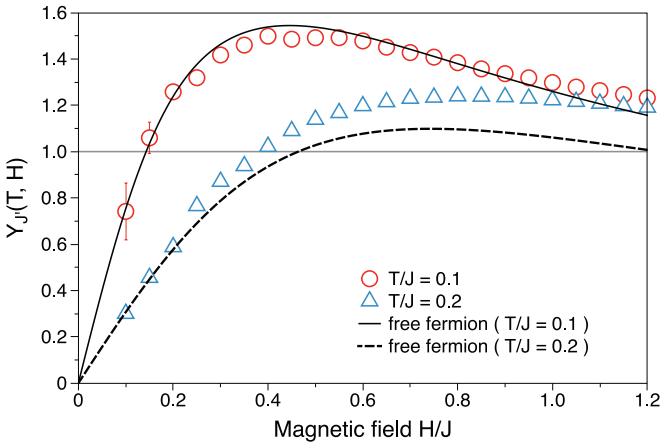

FIG. 7. (Color online) Comparisons of QMC and (A5) at $T/J = 0.1$ and 0.2. The open circles ($T/J = 0.1$) and triangles ($T/J = 0.2$) denote the QMC results. The solid (dashed) curve represents (A5) with $Z_2' = 0.41$ at $T/J = 0.1$ ($T/J = 0.2$).

The coefficient C is a nonuniversal constant. When keeping only the most relevant term $S^a(x)S^a(x+a_0) \sim -S(S+1)n^a(x)n^a(x+a_0)$, we may assume $C > 0$ because the field $\boldsymbol{n}(x)$ is smoothly varying on x. Here, a_0 is the lattice spacing and set to unity. The replacement (A4) immediately leads to $Y_{J'}(T,H) \propto -Y_D(T,H)$ in the infinitesimal field region $H \ll H_{c1}$. This relation is consistent with numerical results (Figs. 1 and 6).

Next, we extend our discussion to the finite-field region $H \sim H_{c1}$ in the exactly same manner with Sec. V. We assume that the replacement (A4) is also valid under not so weak magnetic field $H \sim H_{c1}$. Then, the normalized shift $Y_{J'}(T,H)$ near $H = H_{c1}$ is given by

$$Y_{J'}(T,H) = -\frac{3Z_2'}{2m(T,H)} \int_{-\infty}^{\infty} \frac{dk}{2\pi} [2f_0(k) - f_+(k) - f_-(k)]. \tag{A5}$$

We determine the phenomenological parameter Z_2' by fitting (A5) with QMC data at $T/J = 0.1$. The fitting leads to $Z_2' \approx 0.41$. Figure 7 shows the comparison of (A5) and QMC data for $T/J = 0.1$ and 0.2. The formula (A5) reproduces the QMC data well. But, their agreement rapidly becomes worse as the temperature rises. This discrepancy stems from the saturation value $Y_{J'}(T,H) \to 1$ in the limit $H \to +\infty$. While $Y_D(T,H)$ is negative in the low-field region $H \ll H_{c1}$, $Y_{J'}(T,H)$ is positive there. Thus, the sign change of the normalized shift does not occur for $Y_{J'}(T,H)$. As we have discussed in Sec. VII, this is in contrast to the behavior of $Y_D(T,H)$, which universally shows a sign change.

[1] I. Affleck, Phys. Rev. B **43**, 3215 (1991).
[2] R. Chitra and T. Giamarchi, Phys. Rev. B **55**, 5816 (1997).
[3] M. Klanjšek, H. Mayaffre, C. Berthier, M. Horvatić, B. Chiari, O. Piovesana, P. Bouillot, C. Kollath, E. Orignac, R. Citro, and T. Giamarchi, Phys. Rev. Lett. **101**, 137207 (2008).
[4] E. Čižmár, M. Ozerov, J. Wosnitza, B. Thielemann, K. W. Krämer, C. Rüegg, O. Piovesana, M. Klanjšek, M. Horvatić, C. Berthier, and S. A. Zvyagin, Phys. Rev. B **82**, 054431 (2010).
[5] T. Kashiwagi, M. Hagiwara, S. Kimura, Z. Honda, H. Miyazaki, I. Harada, and K. Kindo, Phys. Rev. B **79**, 024403 (2009).
[6] V. N. Glazkov, A. I. Smirnov, A. Zheludev, and B. C. Sales, Phys. Rev. B **82**, 184406 (2010).
[7] M. Oshikawa and I. Affleck, Phys. Rev. B **65**, 134410 (2002).
[8] M. Brockmann, F. Göhmann, M. Karbach, A. Klümper, and A. Weiße, Phys. Rev. Lett. **107**, 017202 (2011).
[9] M. Brockmann, F. Göhmann, M. Karbach, A. Klümper, and A. Weiße, Phys. Rev. B **85**, 134438 (2012).
[10] Y. Maeda, K. Sakai, and M. Oshikawa, Phys. Rev. Lett. **95**, 037602 (2005).
[11] I. Affleck, Phys. Rev. B **46**, 9002 (1992).
[12] T. Sakai and H. Shiba, J. Phys. Soc. Jpn. **63**, 867 (1994).
[13] S. C. Furuya, T. Suzuki, S. Takayoshi, Y. Maeda, and M. Oshikawa, Phys. Rev. B **84**, 180410 (2011).
[14] D. Controzzi and G. Mussardo, Phys. Rev. Lett. **92**, 021601 (2004).
[15] J. Kanamori and M. Tachiki, J. Phys. Soc. Jpn. **17**, 1384 (1962).
[16] K. Nagata and Y. Tazuke, J. Phys. Soc. Jpn. **32**, 337 (1972).
[17] K. Nagata, J. Phys. Soc. Jpn. **40**, 1209 (1976).
[18] Y. Maeda and M. Oshikawa, J. Phys. Soc. Jpn. **74**, 283 (2005).
[19] S. C. Furuya, P. Bouillot, C. Kollath, M. Oshikawa, and T. Giamarchi, Phys. Rev. Lett. **108**, 037204 (2012).
[20] S. Todo and K. Kato, Phys. Rev. Lett. **87**, 047203 (2001).
[21] F. D. M. Haldane, Phys. Rev. Lett. **50**, 1153 (1983).
[22] F. Haldane, Phys. Lett. A **93**, 464 (1983).
[23] I. Affleck and F. D. M. Haldane, Phys. Rev. B **36**, 5291 (1987).
[24] E. S. Sørensen and I. Affleck, Phys. Rev. B **49**, 13235 (1994).
[25] E. S. Sørensen and I. Affleck, Phys. Rev. B **49**, 15771 (1994).
[26] J. Balog and P. Weisz, Nucl. Phys. B **778**, 259 (2007).

[27]T. Giamarchi, C. Rüegg, and O. Tchernyshyov, Nat. Phys. **4**, 198 (2008).
[28]E. H. Lieb and W. Liniger, Phys. Rev. **130**, 1605 (1963).
[29]E. H. Lieb, Phys. Rev. **130**, 1616 (1963).
[30]I. Affleck, Phys. Rev. B **41**, 6697 (1990).
[31]Y. Maeda, C. Hotta, and M. Oshikawa, Phys. Rev. Lett. **99**, 057205 (2007).
[32]R. M. Konik and P. Fendley, Phys. Rev. B **66**, 144416 (2002).
[33]Z. Honda, H. Asakawa, and K. Katsumata, Phys. Rev. Lett. **81**, 2566 (1998).
[34]A. Zheludev, Y. Chen, C. L. Broholm, Z. Honda, and K. Katsumata, Phys. Rev. B **63**, 104410 (2001).
[35]A. Zheludev, Z. Honda, C. L. Broholm, K. Katsumata, S. M. Shapiro, A. Kolezhuk, S. Park, and Y. Qiu, Phys. Rev. B **68**, 134438 (2003).
[36]J. P. Renard, M. Verdaguer, L. P. Regnault, W. A. C. Erkelens, J. Rossat-Mignod, and W. G. Stirling, Europhys. Lett. **3**, 945 (1987).
[37]A. Escuer, R. Vicente, and X. Solans, J. Chem. Soc. Dalton Trans. (1997) 531.
[38]Z. Honda, K. Katsumata, H. A. Katori, K. Yamada, T. Ohishi, T. Manabe, and M. Yamashita, J. Phys.: Condens. Matter **9**, L83 (1997).
[39]T. Suzuki and S.-i. Suga, Phys. Rev. B **72**, 014434 (2005).
[40]J. Tamaki and M. Oshikawa, Phys. Rev. B **85**, 134431 (2012).
[41]A. Albuquerque, F. Alet, P. Corboz, P. Dayal, A. Feiguin, S. Fuchs, L. Gamper, E. Gull, S. Grtler, A. Honecker, R. Igarashi, M. Krner, A. Kozhevnikov, A. Luchli, S. Manmana, M. Matsumoto, I. McCulloch, F. Michel, R. Noack, G. Pawłowski, L. Pollet, T. Pruschke, U. Schollwck, S. Todo, S. Trebst, M. Troyer, P. Werner, and S. Wessel, J. Magn. Magn. Mater. **310**, 1187 (2007).